J. Fluid Mech. (1977), *vol.* 83, *part* 3, *pp.* 465–493
Printed in Great Britain

Numerical solution of conservation equations arising in linear wave theory: application to aeroacoustics

By SÉBASTIEN M. CANDEL
Office National d'Etudes et de Recherches Aérospatiales (ONERA), and Université de Technologie de Compiègne, 92320 Chatillon, France

(Received 17 January 1977)

The propagation of waves in slightly inhomogeneous dispersive media is conveniently described by a geometrical or kinematic theory. In such frameworks the solution of the propagation problem is constructed by (*a*) deriving a dispersion relation and determining its characteristic lines and (*b*) solving an equation expressing the conservation of a field invariant like the wave action. This paper is concerned with the implementation of the last step under general field and boundary conditions. The method presented is based on the derivation of a variational system of differential equations for the geodesic elements of the wave front. The elementary cross-section of the wave front is obtained by integration and the principle of conservation of the field invariant directly yields the field amplitude. In addition, suitable jump conditions are derived for treating specular reflexions at solid boundaries. The method is illustrated by specific problems of interest in aeroacoustics.

1. Introduction

The propagation of waves in a medium whose characteristic scale l and characteristic time τ greatly exceed the wavelength λ and period $T = 2\pi/\omega$ may be easily described by means of a geometrical theory or in terms of the more recent theory of waves in slightly dispersive, inhomogeneous and nonlinear media. In these formalisms, the solution of the propagation problem is constructed in three steps.

A dispersion relation between the angular frequency ω and the wave vector $\mathbf{k}$ is obtained in the first step. The second step consists of the determination of the characteristic lines or 'rays' of the dispersion relation. Finally, in the third step, the field amplitude is calculated by solving an equation which generally exhibits a conservation form and describes the invariance of a field property like the wave action along the characteristic lines. Depending on the area of physics this equation bears the name of Poynting theorem (electromagnetism), conservation of wave action (fluid mechanics) or adiabatic invariant (particle mechanics).

The rays associated with the dispersion relation are traced in numerous analyses of wave propagation in inhomogeneous media, for instance in the case of electromagnetic waves in the ionosphere, optical beams in graded index fibres, acoustic waves in the atmosphere or the ocean and seismic waves in the ground (see, for example, Quemada 1968; Marcuse 1972; Gossard & Hooke 1975; Urick 1975; Telford *et al.* 1976).

The complete determination of the field (i.e. the third step in the solution construction) is performed in only a more restricted number of studies, and generally

on the basis of either particular analytic expressions or a far-field approximation. Kline (1961) shows, for instance, that it is possible to calculate the field amplitude if one knows the principal curvatures R_1 and R_2 of the wave front along the characteristic trajectories. In this case, the ratio of the intensities I_1 and I_2 at two points of a trajectory may be written as a path integral:

$$\frac{I_2}{I_1} = \exp \int_{s_1}^{s_2} -\left(\frac{1}{R_1}+\frac{1}{R_2}\right) ds. \tag{1}$$

The field amplitude may then be deduced from the intensity. This method is, however, difficult to use in the case of propagation in an inhomogeneous medium, as the curvatures $1/R_1$ and $1/R_2$ are generally unknown.

Another method, extensively used in underwater acoustics, consists of establishing a relation between the field amplitude and the local ray density. After tracing a large number of trajectories in uniformly distributed directions it is possible to estimate this density, for instance by calculating the distance between adjacent rays. This procedure is, however, uneconomical in computation time and its precision diminishes as the range is increased.

Also in relation to underwater propagation, several authors (Ugincius 1969; Solomon & Armijo 1971; Mackinnon, Partridge & Toole 1972) propose calculating the field amplitude by first obtaining the variation of the ray-tube cross-section along each ray. This may be achieved by integrating a set of ordinary differential equations along the characteristic lines. The methods given are, however, specific to underwater applications and consider only an inhomogeneous index. Furthermore, the derivation of differential equations for the ray-tube cross-section seems difficult in the case of propagation in anisotropic media. Nevertheless the ideas presented by Ugincius (1969) are of interest and will be given in a different form in the present paper.

A slightly different track is followed by Chen & Ludwig (1973). Their procedure is based on the formulation of the differential equations for the ray-tube cross-section in terms of intrinsic co-ordinates defined by the ray bundle. A slight reduction in the number of differential equations is obtained in this way but the derivation of the differential system necessitates a considerable amount of algebraic manipulation. The method is also difficult to use in the case of acoustic propagation in a moving medium.

The most complete and general analysis of the problem is given by Hayes (1970) in the context of the 'kinematic' wave theory. Hayes bases the calculation of the field amplitude on the determination of the elementary 'volume convected along the rays', i.e. the volume of a wave packet during its propagation. This volume may be obtained from the Jacobian of the transformation which maps the initial parameter space onto the 'augmented' space of positions along the ray (i.e. the space formed by the couples (position; time) along each ray). The Jacobian is in turn obtained by integrating a system of differential equations derived from the characteristic system. Hayes specializes his method to the case of acoustic propagation in a stratified medium and uses a numerical algorithm developed by Hayes, Haefli & Kulsrud (1970) to calculate the sonic boom in a stratified atmosphere.

The method developed in the present paper is a variant of that proposed by Hayes (1970) and borrows some ideas from Ugincius (1969).

The conservation equation is solved by calculating the variation of *the elementary*

wave-front section along each ray. The ray-tube cross-section is then obtained indirectly from the wave-front section. Indeed a direct calculation of the ray-tube cross-section would require the derivation of a complicated system of differential equations. In contrast, the differential equations defining the wave front may be instantly deduced from the characteristic system.

The method is first presented (§3) for the case of an infinite medium and then extended in §6 to the case where reflecting boundaries exist in the domain. This situation, important in numerous applications, is not considered by Hayes (1970) and complicated methods are generally developed to treat this problem (see Friedlander 1958). We show that a certain set of jump conditions may be used to re-initiate the numerical integration when the characteristic trajectory is specularly reflected.

The general method is specialized to the case of acoustic propagation in §§4 and 5 and three examples of interest in the aeroacoustic domain are treated to illustrate the power of the geometrical theory when it is implemented through a numerical algorithm (§7). The paper begins with a rapid outline of the basic results of the geometrical formalism.

2. Basic results of the geometrical theory of propagation

We refer the reader to classical textbooks and papers (e.g. Whitham 1974; Felsen & Marcuvitz 1973; Born & Wolf 1975) or to Candel (1976*b*) for a more detailed presentation of the geometrical formalism. The main steps and results are worth summarizing.

The basic problem is to construct the solution of a system of equations of the form

$$L(\nabla, \partial/\partial t; \mathbf{x}, t)\,\mathbf{u}(\mathbf{x}, t) = 0. \tag{2}$$

The solution is cast in the form of a local plane wave

$$\mathbf{u}(\mathbf{x}, t) = \mathbf{u}^0(\mathbf{x}, t)\, e^{i\psi(\mathbf{x}, t)}, \tag{3}$$

where $\mathbf{u}^0(\mathbf{x}, t)$ is an amplitude vector and $\psi(\mathbf{x}, t)$ a phase function. In analogy with wave propagation in homogeneous media, one defines a local wave vector

$$\mathbf{k} = \nabla\psi \tag{4}$$

and a local angular frequency $$\omega = -\partial\psi/\partial t. \tag{5}$$

Expression (3) is then substituted in the system of equations (2) and the amplitude vector is expanded in an asymptotic series

$$\mathbf{u}^0 = \mathbf{u}_0 + \mathbf{u}_1 + \mathbf{u}_2 + \ldots. \tag{6}$$

The successive terms are ordered such that

$$\|u_n(\mathbf{x}, t)\| / \|\mathbf{u}_{n-1}(\mathbf{x}, t)\| = O(\epsilon),$$

where ϵ designates a small parameter of the order of the ratio of the wavelength to the characteristic length scale or of the period to the characteristic time scale of the medium.

This procedure yields at zeroth order a dispersion relation $D(\omega, \mathbf{k}; \mathbf{x}, t) = 0$ which may be cast in the form

$$\omega = \Omega(\mathbf{k}, \mathbf{x}, t). \tag{7}$$

The next orders lead to equations which may generally be written as

$$\partial A_n/\partial t + \nabla . \mathbf{c}_g A_n = f(\mathbf{u}_{n-1}), \tag{8}$$

where $\mathbf{c}_g$ designates the group velocity

$$\mathbf{c}_g = \partial\Omega/\partial\mathbf{k} \tag{9}$$

and A_n is the 'wave action' associated with the $\mathbf{u}_n$ term of the geometrical expansion (6):

$$A_n = A_n(\mathbf{u}_n, \omega, \mathbf{k}; \mathbf{x}, t). \tag{10}$$

In a number of cases the first of equations (8), describing $\mathbf{u}_0(\mathbf{x}, t)$, takes a conservation form

$$\partial A_0/\partial t + \nabla . \mathbf{c}_g A_0 = 0. \tag{11}$$

The dispersion relation (7) is conveniently solved by the method of characteristics, i.e. by tracing the rays defined by

$$\frac{d^c\mathbf{x}}{dt} = \frac{\partial\Omega}{\partial\mathbf{k}}, \quad \frac{d^c\mathbf{k}}{dt} = -\nabla\Omega, \quad \frac{d^c\omega}{dt} = \frac{\partial\Omega}{\partial t}, \tag{12}$$

where d^c/dt represents differentiation along the characteristic lines, i.e.

$$d^c/dt = \partial/\partial t + \mathbf{c}_g . \nabla. \tag{13}$$

The phase is then obtained from the additional equation

$$d^c\psi/dt = -\Omega + \mathbf{k} . \partial\Omega/\partial t. \tag{14}$$

We are here concerned with the solution of the conservation equation (11). A first step in that direction consists of showing that the action contained in a wave packet is conserved along each characteristic line (Whitham 1974, p. 389). To this end let us consider the total action contained in a 'wave volume' $\mathscr{V}(t)$ (a volume propagating at the group velocity along the space–time rays as shown on figure 1; the wave volume is analogous to the material volume of fluid mechanics):

$$\int_{\mathscr{V}(t)} A_0 d\mathscr{V}. \tag{15}$$

The variation of this quantity with respect to time may be obtained through the integral transport identity

$$\frac{d}{dt}\int_{\mathscr{V}(t)} A_0 d\mathscr{V} = \int_{\mathscr{V}(t)} \frac{\partial A_0}{\partial t} d\mathscr{V} + \int_{a(t)} A_0 \mathbf{c}_g . \mathbf{da}. \tag{16}$$

Application of Green's theorem and use of the local equation (11) leads to

$$\frac{d}{dt}\int_{\mathscr{V}(t)} A_0 d\mathscr{V} = 0, \tag{17}$$

which expresses the fact that the action contained in a wave volume is invariant.

By specializing (17) to an elementary wave volume or wave packet

$$d\mathscr{V} = c_g \delta a dt, \tag{18}$$

one finds that

$$A_0 c_g \delta a = \text{constant} \tag{19}$$

along the characteristic lines.

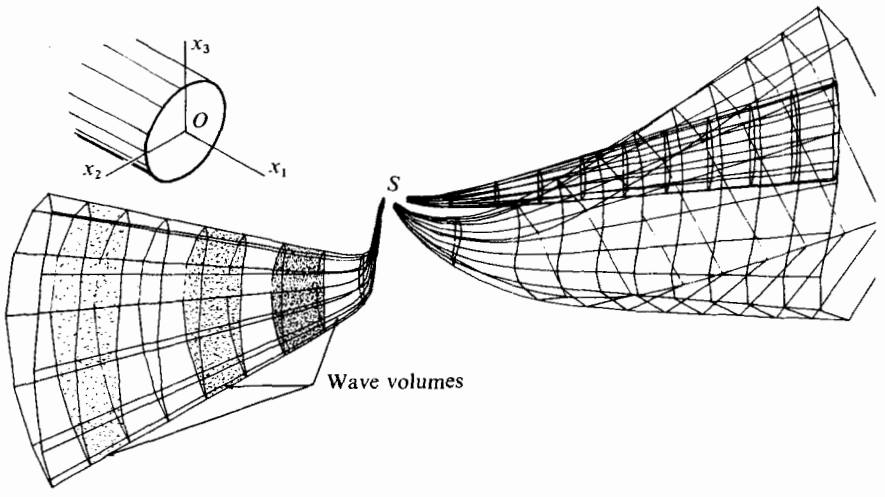

FIGURE 1. Ray tubes and wave volumes.

Now this invariance property is useful in practice if it is possible to calculate the variation of the elementary ray-tube cross-section δa along the ray. The analysis of this problem is pursued in the next section. However, first it is worth describing the formalism which has been classically used in the case of time-independent media. There the solution is written in the form

$$\mathbf{u}(\mathbf{x}, t) = \mathbf{u}^0(\mathbf{x}) \exp\{ik_0 S(\mathbf{x}) - i\omega t\}, \tag{20}$$

where the angular frequency ω is constant in the domain. The dispersion relation is replaced by an Eikonal equation generally written in the form

$$H(\mathbf{x}, \nabla S) = H(\mathbf{x}, \mathbf{p}) = 0. \tag{21}$$

The ray equations solving (21) become

$$d^c\mathbf{x}/d\tau = \partial H/\partial \mathbf{p}, \quad d^c\mathbf{p}/d\tau = -\partial H/\partial \mathbf{x} \tag{22}$$

and the phase is given by $$d^cS/d\tau = \mathbf{p}.\partial H/\partial \mathbf{p}. \tag{23}$$

The conservation equation (11) then reduces to

$$\nabla.\mathbf{c}_g A_0 = 0. \tag{24}$$

To fix ideas and allow better comprehension of §4, we have summarized the basic results of the geometrical acoustics theory in appendices A and B.

3. Description of the solution method

Variational system of equations

We have just seen that a conservation equation of the form (11) could be solved by calculating the variation of the elementary ray-tube cross-section along the ray line. We also pointed out, in the introduction, that this calculation is rendered difficult when the medium is anisotropic. We propose instead to evaluate the elementary cross-section $\delta\Sigma$ of the wave front and then deduce δa by using the relation

$$\delta a = \delta\Sigma \cos(\boldsymbol{\nu}, \hat{\mathbf{x}}), \tag{25}$$

where $\boldsymbol{\upsilon}$ designates a unit vector in the wave-vector direction and $\hat{\mathbf{x}}$ is a unit vector in the ray direction.

Now to calculate $\delta\Sigma$ we are going to develop a system of differential equations for the geodesic elements of the wave front. We start from the characteristic system defining the characteristic trajectories for the medium under consideration. If the medium is time independent the characteristic system is autonomous and may be cast in the general form

$$d\mathbf{x}/dS = \mathbf{f}(\mathbf{x}, \mathbf{p}), \quad d\mathbf{p}/dS = \mathbf{g}(\mathbf{x}, \mathbf{p}). \tag{26}$$

The phase parameter does not appear on the right-hand side. The system requires five initial conditions, the sixth being obtained from the Eikonal equation

$$H(\mathbf{x}, \mathbf{p}) = 0. \tag{27}$$

When the medium is time dependent the characteristic system is not autonomous and an additional equation determines the local angular frequency:

$$d\mathbf{x}/dt = \mathbf{f}(\mathbf{x}, \mathbf{k}, t), \quad d\mathbf{k}/dt = \mathbf{g}(\mathbf{x}, \mathbf{k}, t), \quad d\omega/dt = h(\mathbf{x}, \mathbf{k}, t). \tag{28}$$

Six initial conditions are then required, the seventh being deduced from the dispersion relation

$$D(\omega, \mathbf{k}; \mathbf{x}, t) = 0 \tag{29}$$

or

$$\omega = \Omega(\mathbf{x}, \mathbf{k}, t). \tag{30}$$

One is generally concerned with families of ray lines having a reduced space of initial parameters. For instance one may consider the ray bundle radiated from a fixed source situated at $\mathbf{x}_0$. Then for a time-independent medium the ray lines are a function of two initial parameters such as the angles θ_0 and α_0 defining the initial wave vector. For a fixed source in a time-dependent medium the rays form a family with three initial parameters.

For the sake of simplicity let us consider the time-independent situation. The position vector $\mathbf{x}$ and the wave vector $\mathbf{p}$ of a current point on the ray line are completely determined by the value of the phase parameter S and the initial angles θ_0 and α_0:

$$\mathbf{x} = \mathbf{x}(S, \theta_0, \alpha_0), \quad \mathbf{p} = \mathbf{p}(S, \theta_0, \alpha_0). \tag{31), (32}$$

Another interesting situation is that where the position of an 'initial' wave front is known. The wave front may be represented by an equation of the form

$$S_0(\mathbf{x}) = 0, \tag{33}$$

or more conveniently, in terms of two initial parameters λ_0 and μ_0 which define a two-dimensional subspace

$$\mathbf{x}(0) = \mathbf{x}_0(\lambda_0, \mu_0). \tag{34}$$

At these points, the unit wave vector is defined by

$$\boldsymbol{\nu} = \frac{\partial \mathbf{x}_0}{\partial \lambda_0} \times \frac{\partial \mathbf{x}_0}{\partial \mu_0} \Big/ \left| \frac{\partial \mathbf{x}_0}{\partial \lambda_0} \times \frac{\partial \mathbf{x}_0}{\partial \mu_0} \right| = \boldsymbol{\nu}(\lambda_0, \mu_0) \tag{35}$$

and depends uniquely on the parameters λ_0 and μ_0. Thus the position and wave vectors $\mathbf{x}$ and $\mathbf{p}$ on a ray originating from the initial wave front S_0 depend only on the two initial parameters λ_0 and μ_0 and on the current value of the phase S.

In the remainder of this paper we designate the two initial parameters by θ_0 and

α_0 and the phase by S. We also specifically consider the time-independent case but note that a similar argument applies to the time-dependent situation.

Now the elementary phase front may be computed from the local geodesic elements

$$\mathbf{R}^\theta = (\partial \mathbf{x}/\partial\theta_0)_{S,\alpha_0}, \quad \mathbf{R}^\alpha = (\partial \mathbf{x}/\partial\alpha_0)_{S,\theta_0} \tag{36}$$

through a vectorial product: $$\boldsymbol{\delta\Sigma} = \mathbf{R}^\theta \times \mathbf{R}^\alpha d\theta_0 d\alpha_0. \tag{37}$$

The problem reduces to the determination of the geodesic elements of the wave front along the ray line. These elements are solutions of a system of differential equations which may be obtained by taking variations of the characteristic system with respect to the initial parameters θ_0 and α_0 while keeping the phase constant. This procedure directly yields

$$\frac{d\mathbf{R}}{dS} = \frac{\partial \mathbf{f}}{\partial \mathbf{x}}.\mathbf{R} + \frac{\partial \mathbf{f}}{\partial \mathbf{p}}.\mathbf{Q}, \tag{38a}$$

$$\frac{d\mathbf{Q}}{dS} = \frac{\partial \mathbf{g}}{\partial \mathbf{x}}.\mathbf{R} + \frac{\partial \mathbf{g}}{\partial \mathbf{p}}.\mathbf{Q}, \tag{38b}$$

where $\mathbf{Q}$ designates 'conjugate' elements defined by

$$\mathbf{Q}^\theta = \partial \mathbf{p}/\partial\theta_0, \quad Q^\alpha = \partial \mathbf{p}/\partial\alpha_0. \tag{39}$$

Very often, the wave-vector modulus appears explicitly in the characteristic system. Its variation with respect to the initial parameters is obtained by differentiating $p = (\mathbf{p}.\mathbf{p})^{\frac{1}{2}}$:

$$\partial p/\partial\theta_0 = \boldsymbol{\nu}.\mathbf{Q}^\theta. \tag{40}$$

This expression will also be used in the next subsection.

Initial conditions (fixed source)

The differential system (38) requires appropriate initial conditions, which we are now going to derive. To obtain the initial geodesic elements $\mathbf{R}^\theta(0)$ and $\mathbf{R}^\alpha(0)$ we expand the position vector as a Taylor series near the origin,

$$\mathbf{x}(S) = \mathbf{x}(0) + S\mathbf{f}(\mathbf{x}(0), \mathbf{p}(0)) + O(S^2), \tag{41}$$

and then differentiate this expression with respect to the initial parameter θ_0 or α_0. This yields

$$\mathbf{R}^\theta(0) = \lim_{s\to 0} \frac{\partial \mathbf{x}}{\partial\theta_0} = \lim_{s\to 0} S\left[\frac{\partial \mathbf{f}}{\partial \mathbf{x}}(0).\mathbf{R}^\theta(0) + \frac{\partial \mathbf{f}}{\partial \mathbf{p}}(0).\mathbf{Q}^\theta(0)\right] \tag{42}$$

and a similar expression for $\mathbf{R}^\alpha(0)$. The term contained in the brackets is generally bounded and the geodesic elements vanish at the origin:

$$\mathbf{R}^\theta(0) = \mathbf{R}^\alpha(0) \equiv 0 \tag{43}$$

(as the ray tube reduces to a point at the source, this result could have been anticipated).

Now a similar argument provides $\mathbf{Q}^\theta(0)$ and $\mathbf{Q}^\alpha(0)$. We start from

$$\mathbf{p}(S) = \mathbf{p}(0) + S\mathbf{g}(\mathbf{x}(0), \mathbf{p}(0)) + O(S^2) \tag{44}$$

and obtain

$$Q^\theta(0) = \frac{\partial \mathbf{p}(0)}{\partial\theta_0} = \frac{\partial p(0)}{\partial\theta_0}\boldsymbol{\nu}_0 + p(0)\frac{\partial \boldsymbol{\nu}_0}{\partial\theta_0}, \tag{45}$$

or by substituting (40) in (45),

$$\mathbf{Q}^{\theta}(0) = [\mathbf{I} - \boldsymbol{\nu}_0 \boldsymbol{\nu}_0]^{-1} . \frac{\partial \boldsymbol{\nu}_0}{\partial \theta_0} p(0). \tag{46}$$

In summary, the geodesic elements defining the elemental wave-front area may be calculated by integrating twelve ordinary differential equations in addition to the six characteristic equations. Five initial conditions are required (e.g. the source position and two initial wave-vector angles), the other conditions being determined as shown above.

Theoretical considerations

The method proposed resembles the parameter differentiation procedure used to solve two-point boundary-value problems and also the sensitivity analysis of first-order differential systems. All these methods are founded on classical theorems of the theory of differential equations and it is worth recalling some of these results. We refer the reader to Struble (1962) for a detailed account.

We here consider systems of equations of autonomous or non-autonomous type which may be cast in the general form

$$d\mathbf{x}/dt = \mathbf{f}(\mathbf{x}, \boldsymbol{\alpha}, t), \quad \mathbf{x}(0) = \mathbf{c}, \tag{47), (48}$$

where $\boldsymbol{\alpha}$ represents a set of j parameters. For such systems one can show the following.

(i) A solution exists in the neighbourhood of $t = 0$ if $\mathbf{f}$ is a continuous function of $\mathbf{x}$ and t and satisfies certain Lipshitz-type conditions.

(ii) This solution has kth-order continuous derivatives in the variables $\boldsymbol{\alpha}$ and $\mathbf{c}$ if $\mathbf{f}$ has kth-order continuous derivatives in the $j+n+1$ variables comprising $\boldsymbol{\alpha}$, $\mathbf{x}$ and t.

Furthermore the matrix

$$\mathbf{X} = \partial \mathbf{x}/\partial \mathbf{c} \tag{49}$$

obtained by differentiating the solution of system (48) with respect to the set of initial conditions satisfies the matrix equation

$$\frac{d\mathbf{X}}{dt} = \frac{\partial \mathbf{f}}{\partial \mathbf{x}}(\mathbf{x}, \boldsymbol{\alpha}, t)\, \mathbf{X}, \tag{50}$$

where $\partial \mathbf{f}/\partial \mathbf{x}$ is the Jacobian matrix and $|\mathbf{X}|$ the determinant (or Jacobian) of the transformation which maps the initial vector space defined by $\mathbf{c}$ onto the position vector $\mathbf{x}(t)$. The columns of this matrix may be identified as the geodesic elements of this mapping.

The system derived in the previous subsection for the geodesic elements of the wave front is just the restriction of (50) to the two-dimensional space defined by the initial parameters θ_0 and α_0. The matrix $\mathbf{X}$ has in that case two rows and six columns and (50) represents twelve differential equations.

The significance of the variational system (38) may be clarified if one refers to the principle of conservation of the wave action transported by a wave packet:

$$A_0 d\mathscr{V} = \text{constant}. \tag{51}$$

In this expression the wave-packet volume $d\mathscr{V}$ may be evaluated from the Jacobian of the transformation which maps θ_0, α_0 and t onto the position vector $\mathbf{x}$:

$$d\mathscr{V} = \frac{D(x_1, x_2, x_3)}{D(\theta_0, \alpha_0, t)}\, d\alpha_0 d\theta_0 dt. \tag{52}$$

The first two rows of this Jacobian are the geodesic elements $\mathbf{R}^\theta$ and $\mathbf{R}^\alpha$ and the components of the group velocity appear in the third row, so that

$$d\mathscr{V} = \mathbf{c}_g . \mathbf{R}^\theta \times \mathbf{R}^\alpha d\theta_0 d\alpha_0 dt, \tag{53}$$

or

$$d\mathscr{V} = \mathbf{c}_g . \boldsymbol{\delta\Sigma} dt = c_g \delta a dt. \tag{54}$$

This indicates that the Jacobian may be calculated from the elemental wave-front area, and the conservation principle (51) then directly yields the field amplitude.

The preceding theorems show that the characteristic system possesses a solution in a neighbourhood of the origin. Under certain conditions, differentiation of this system with respect to the initial set of parameters is justified and the resulting equations define a transformation between the initial parameter space and the current wave front and allow the calculation of the elementary wave-front cross-section $\delta\Sigma$.

Accuracy and validity of the method

An aspect which is worth underlining is the existence of two criteria allowing an estimation of the accuracy of the numerical solution. The first criterion consists of verifying that the characteristic system indeed provides a solution of the Eikonal equation (or of the dispersion relation). In the case of acoustic propagation (see next sections) we actually compare the wave-vector modulus obtained by integration with the modulus given by the Eikonal equation:

$$p = N/(1 + \mathbf{M} . \boldsymbol{\nu}), \tag{55}$$

where $\mathbf{M}$ is the Mach number vector. The second criterion concerns the calculation of $\boldsymbol{\delta\Sigma}$. The elemental area is determined vectorially by its three components. It is possible to verify that the vector obtained is parallel to the direction of the local wave vector. For this purpose it is sufficient to form the ratio

$$|\delta\Sigma - \boldsymbol{\delta\Sigma} . \boldsymbol{\nu}|/\delta\Sigma \tag{56}$$

and verify that its value remains almost zero.

Indeed in all cases treated with the geometrical acoustics algorithm this ratio was found to be smaller than 10^{-3} for an integration step $\delta S/D = 0{\cdot}04$ (D represents a characteristic geometric scale like the initial diameter of a jet flow). Very often the medium of propagation changes on a scale l which may be smaller than D and the ratio $\delta S/l$ of the integration step to this scale would reach values of the order of 0·3. The precision of the integration (performed with a fourth-order Runge–Kutta procedure) is nevertheless maintained.

4. Acoustic propagation in an inhomogeneous moving medium

We now specialize the general method to the case of acoustic wave propagation in an inhomogeneous medium in steady motion.

Variational system

The characteristic system becomes in this case (appendix B)

$$d\mathbf{x}/dS = N^{-1}(\boldsymbol{\nu} + \mathbf{M}), \tag{57a}$$

$$d\mathbf{p}/dS = N^{-1}[\nabla N - (\nabla \mathbf{M}) . \mathbf{p}]. \tag{57b}$$

Taking the variations of this system with respect to one of the initial parameters gives

$$\frac{d\mathbf{R}}{dS} = \frac{1}{pN}(\mathbf{Q} - \boldsymbol{\nu}\boldsymbol{\nu}.\mathbf{Q}) - \frac{(\mathbf{M}+\boldsymbol{\nu})}{N^2}(\mathbf{R}.\nabla N) + \frac{1}{N}(\mathbf{R}.\nabla\mathbf{M}), \tag{58a}$$

$$\frac{d\mathbf{Q}}{dS} = \frac{1}{N}[\mathbf{R}.\nabla\nabla N - \mathbf{R}.(\nabla\nabla\mathbf{M}).\mathbf{p} - (\nabla\mathbf{M}).\mathbf{Q}] - \frac{1}{N^2}(\mathbf{R}.\nabla N)[\nabla N - (\nabla\mathbf{M}).\mathbf{p}]. \tag{58b}$$

Some ambiguities arise in the vectorial notation used in the preceding expressions so it is worth giving the indicial form of these equations:

$$\frac{dR_i}{dS} = \frac{1}{pN}(Q_i - \nu_i\nu_j Q_j) - \frac{(M_i+\nu_i)}{N^2}R_j\partial_j N + \frac{1}{N}R_j\partial_j M_i, \tag{59a}$$

$$\frac{dQ_i}{dS} = \frac{1}{N}[R_j\partial_j\partial_i N - R_j(\partial_j\partial_i M_k)p_k - Q_j\partial_i M_j] - \frac{1}{N^2}R_j\partial_j N[\partial_i N - p_k\partial_i M_k]. \tag{59b}$$

The first three equations of this system give the rate of variation of the geodesic element $\mathbf{R}$ and involve only first-order derivatives of the Mach number and index. The last three equations define the conjugate elements and require second-order derivatives of the local properties N and $\mathbf{M}$.

Initial conditions

We consider the case of acoustic radiation from a point source and specialize the general set of initial conditions given in § 3 to this particular situation.

We already know that the geodesic elements vanish at the source:

$$\mathbf{R}^\theta(0) = \mathbf{R}^\alpha(0) = 0. \tag{60}$$

To get the conjugate elements $\mathbf{Q}^\theta(0)$ and $\mathbf{Q}^\alpha(0)$ we may resort to expression (45), which we are now going to write out more explicitly. First we choose a Cartesian system x_1 axis is parallel to the flow direction at the source. The unit vector $\boldsymbol{\nu}_0$ in the direction of the initial wave vector has components

$$\nu_{01} = \cos\theta_0, \quad \nu_{02} = \sin\theta_0\cos\alpha_0, \quad \nu_{03} = \sin\theta_0\sin\alpha_0 \tag{61}$$

and the Eikonal equation at the origin is independent of the angle α_0:

$$p(0) = N_0/(1 + M_0\cos\theta_0). \tag{62}$$

Then the initial components of the conjugate elements $\mathbf{Q}^\theta$ and $\mathbf{Q}^\alpha$ are

$$\left.\begin{aligned}
Q_1^\theta(0) &= p_0^2 M_0 \sin\theta_0\cos\theta_0/N_0 - p_0\sin\theta_0,\\
Q_2^\theta(0) &= p_0^2 M_0 \sin^2\theta_0\cos\alpha_0/N_0 + p_0\cos\theta_0\cos\alpha_0,\\
Q_3^\theta(0) &= p_0^2 M_0 \sin^2\theta_0\sin\alpha_0/N_0 + p_0\cos\theta_0\sin\alpha_0,\\
Q_1^\alpha(0) &= 0,\\
Q_2^\alpha(0) &= -p_0\sin\theta_0\sin\alpha_0,\\
Q_3^\alpha(0) &= p_0\sin\theta_0\cos\alpha_0.
\end{aligned}\right\} \tag{63}$$

Numerical implementation

The calculation of the acoustic field reduces to the integration of a system of 18 differential equations formed by the six characteristic equations, six variational equations for the direction θ_0 and the corresponding six equations for the direction α_0.

Initial conditions for the numerical integration are obtained by giving the source position $\mathbf{x}_0$ and the initial wave-vector angles θ_0 and α_0. The Eikonal equation then yields the wave-vector modulus at the source. The other initial values are obtained from expressions (60) and (63). The numerical algorithm used to implement this procedure is also able to account for reflexions at solid boundaries. This is achieved by interrupting the numerical integration when the ray reaches a solid boundary. Upon this occurrence a set of jump conditions (see §6) is used and provides the new values of all the variables. The numerical integration may then proceed until the next reflexion occurs.

5. Acoustic propagation in an inhomogeneous medium at rest

In §4 we established the system of equations which allows the calculation of the geometric acoustic field propagating in an inhomogeneous medium in steady motion. In certain important applications the medium may be considered to be at rest and it is therefore worth restating the system of equations in this particular situation.

The characteristic system becomes in this case

$$d\mathbf{x}/dS = \boldsymbol{\nu}/N, \quad d\mathbf{p}/dS = \nabla N/N \tag{64}$$

and the variational system becomes

$$\frac{d\mathbf{R}}{dS} = \frac{\mathbf{Q}}{N^2} - \frac{2\boldsymbol{\nu}}{N^2}(\mathbf{R}.\nabla N), \tag{65a}$$

$$\frac{d\mathbf{Q}}{dS} = \frac{1}{N}\mathbf{R}.\nabla\nabla N - \frac{1}{N^2}(\mathbf{R}.\nabla N)\nabla N. \tag{65b}$$

The initial conditions also simplify:

$$\mathbf{R}^\theta(0) = \mathbf{R}^\alpha(0) \equiv 0, \tag{66a}$$

$$\mathbf{Q}^\theta(0) = N_0 \partial\boldsymbol{\nu}_0/\partial\theta_0, \quad \mathbf{Q}^\alpha(0) = N_0 \partial\boldsymbol{\nu}_0/\partial\alpha_0. \tag{66b}$$

The system formed by (64) and (65) together with initial conditions (66) allows the calculation of the geometric acoustic field in a medium at rest whose index N is a function of the three spatial co-ordinates.

This extends the classical treatments of the problem, which are in general based on the assumption that the medium is stratified in the vertical direction.

6. Reflexion at solid boundaries

In a large number of practical problems, the propagation medium contains (or is surrounded by) solid boundaries which partially or totally reflect incident waves. In underwater acoustics, for example, reflexions off the ocean bottom or surface are of key importance.

We analyse in this section the problem of specular reflexion in the case of boundaries of arbitrary shape imbedded in an inhomogeneous moving medium. We assume that the reflexion may be treated in the geometrical framework and this implies that the principal radii of curvature are large compared with the wavelength.

Before starting it is worth noting that classical treatments of reflexion generally

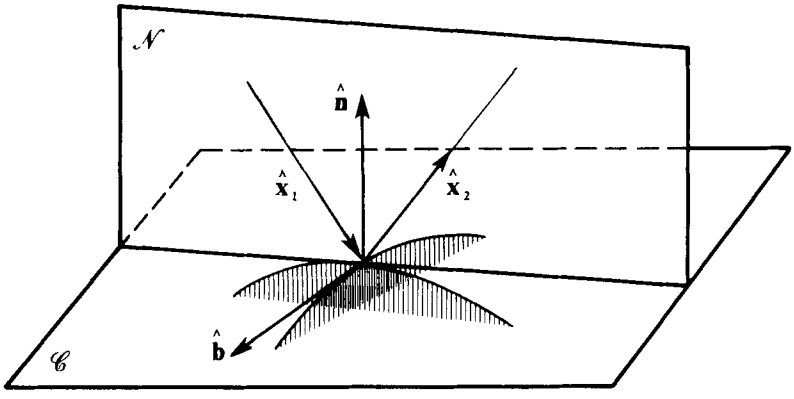

FIGURE 2. Reflexion geometry.

consider the propagation medium to be homogeneous and at rest and are based on analytical expressions for the ray-tube expansion. This approach is exemplified by Friedlander (1958) and Fock (1965). Such a method is difficult to use in the case of an inhomogeneous moving medium and besides it does not allow a simple algorithmic implementation.

Our treatment is essentially different from the classical approach. It is based on the derivation of 'jump' conditions to account for the discontinuities associated with the specular reflexion of the characteristic trajectories. The jump relations serve to re-initiate the numerical integration, which has to be interrupted upon reflexion. The method has some resemblance to the shock-fitting procedure of wave physics for a shock whose position is known in advance.

It is worth starting by detailing the geometry of the problem (figure 2): $\hat{\mathbf{n}}$ designates the unit normal to the surface $\mathscr{D}$ at the reflexion point B, $\mathscr{N}$ is the plane formed by the incident ray and the normal $\hat{\mathbf{n}}$, $\mathscr{C}$ designates the tangent plane at B and $\hat{\mathbf{b}}$ is a unit vector lying in the $\mathscr{C}$ plane and normal to $\mathscr{N}$ at B.

Jump condition for the unit wave and ray vectors

The wave vector is specularly reflected, so that its normal component reverses (or flips) while its tangential projection on $\mathscr{C}$ is conserved:

$$\boldsymbol{\nu}_1 . \hat{\mathbf{n}} = -\boldsymbol{\nu}_2 . \hat{\mathbf{n}}, \tag{67}$$

$$\boldsymbol{\nu}_1 - (\hat{\mathbf{n}} . \boldsymbol{\nu}_1)\hat{\mathbf{n}} = \boldsymbol{\nu}_2 - (\hat{\mathbf{n}} . \boldsymbol{\nu}_2)\hat{\mathbf{n}}. \tag{68}$$

When combined these expressions yield

$$\boldsymbol{\nu}_2 = \boldsymbol{\nu}_1 - 2(\boldsymbol{\nu}_1 . \hat{\mathbf{n}})\hat{\mathbf{n}}. \tag{69}$$

If square brackets are used to denote a discontinuity the preceding expression becomes

$$[\boldsymbol{\nu}] = -2(\boldsymbol{\nu}_1 . \hat{\mathbf{n}})\hat{\mathbf{n}}. \tag{70}$$

The unit wave vector after reflexion is obtained by subtracting from the incident unit wave vector twice its component in the normal direction.

The jump condition for the unit ray vector may be derived from expression (69). For this we note that the flow velocity vector is tangential to the solid boundary (we

assume for the moment that the velocity remains finite at the wall and postpone the discussion of the influence of the boundary-layer structure to the end of this section). In consequence the projection of the unit wave vector on the velocity vector remains invariant, so that

$$|\boldsymbol{\upsilon}_1 + \mathbf{M}| = |\boldsymbol{\upsilon}_2 + \mathbf{M}|. \tag{71}$$

Adding the Mach number vector to both sides of (69) and then dividing by (71) leads to

$$\frac{\boldsymbol{\nu}_2 + \mathbf{M}}{|\boldsymbol{\nu}_2 + \mathbf{M}|} = \frac{\boldsymbol{\nu}_1 + \mathbf{M}}{|\boldsymbol{\nu}_1 + \mathbf{M}|} - 2\left(\frac{\boldsymbol{\nu}_1 + \mathbf{M}}{|\boldsymbol{\nu}_1 + \mathbf{M}|} . \hat{\mathbf{n}}\right)\hat{\mathbf{n}}, \tag{72}$$

or

$$\hat{\boldsymbol{\chi}}_2 = \hat{\boldsymbol{\chi}}_1 - 2(\hat{\boldsymbol{\chi}}_1 . \hat{\mathbf{n}})\hat{\mathbf{n}}. \tag{73}$$

The unit ray vector exhibits the same type of discontinuity as the unit wave vector.

Conditions for the geodesic and conjugate elements

To derive the condition for the geodesic element $\mathbf{R}$ we first decompose this vector into its projection $\mathbf{R}_{\mathscr{N}}$ on the normal plane and R_b on the vector $\hat{\mathbf{b}}$:

$$\mathbf{R} = \mathbf{R}_{\mathscr{N}} + R_b\hat{\mathbf{b}}. \tag{74}$$

Since $\mathbf{R}$ and $\hat{\mathbf{b}}$ are both perpendicular to the wave vector the projection

$$\mathbf{R}_{\mathscr{N}} = \mathbf{R} - (\mathbf{R} . \hat{\mathbf{b}})\hat{\mathbf{b}} \tag{75}$$

is also normal to the wave vector. This component undergoes specular reflexion with its modulus conserved:

$$\mathbf{R}_{\mathscr{N}2} = \mathbf{R}_{\mathscr{N}1} - 2(\mathbf{R}_{\mathscr{N}1} . \hat{\mathbf{n}})\hat{\mathbf{n}}. \tag{76}$$

Turning now to the R_b component, it is easy to see that this remains invariant, so that

$$R_{b2} = R_{b1}. \tag{77}$$

By adding these two expressions we get

$$\mathbf{R}_2 = \mathbf{R}_1 - 2(\mathbf{R}_1 . \hat{\mathbf{n}})\hat{\mathbf{n}}. \tag{78}$$

Thus we see that the geodesic elements 'jump' like the unit wave and ray vectors.

The derivation of the jump relation for the conjugate element is a little more complicated. It is first useful to note that the wave-vector modulus is a conserved quantity:

$$p_2 - p_1 = \frac{N}{1 + \mathbf{M} . \boldsymbol{\nu}_2} - \frac{N}{1 + \mathbf{M} . \boldsymbol{\nu}_1} = 0. \tag{79}$$

We may therefore multiply both sides of (77) by the wave-vector modulus at point B:

$$\mathbf{p}_2 = \mathbf{p}_1 - 2(\mathbf{p}_1 . \hat{\mathbf{n}})\hat{\mathbf{n}}. \tag{80}$$

Taking the variation of this expression with respect to one of the initial parameters (for instance θ_0) yields

$$\mathbf{Q}_2^{\varrho} = \mathbf{Q}_1^{\varrho} - 2(\mathbf{Q}_1^{\varrho} . \hat{\mathbf{n}})\hat{\mathbf{n}} - 2\mathbf{p}_1 . \frac{\partial \hat{\mathbf{n}}\hat{\mathbf{n}}}{\partial \mathbf{x}} . \left(\frac{\partial \mathbf{x}}{\partial \theta_0}\right)_{\mathscr{D}}. \tag{81}$$

The variation of $\mathbf{x}$ associated with the variation of the initial parameter appears in the last term. To get an expression for $(\partial \mathbf{x}/\partial \theta_0)_{\mathscr{D}}$ we note that the reflexion points lie on the solid surface $\mathscr{D}$ and satisfy

$$G(\mathbf{x}(\theta_0, \alpha_0, S)) = 0. \tag{82}$$

The parameters α_0, θ_0 and S are therefore not independent and thus

$$\left(\frac{\partial \mathbf{x}}{\partial \theta_0}\right)_{\mathscr{D}} = \left(\frac{\partial \mathbf{x}}{\partial \theta_0}\right)_{\alpha_0, S} + \left(\frac{\partial \mathbf{x}}{\partial S}\right)_{\alpha_0, \theta_0} \frac{\partial S}{\partial \theta_0}. \tag{83}$$

In addition differentiation of (90) yields

$$\hat{\mathbf{n}}.\left[\left(\frac{\partial \mathbf{x}}{\partial \theta_0}\right)_{\alpha_0, S} + \left(\frac{\partial \mathbf{x}}{\partial S}\right)_{\alpha_0, \theta_0} \frac{\partial S}{\partial \theta_0}\right] = 0. \tag{84}$$

On combining (83) and (84) we get

$$\left(\frac{\partial \mathbf{x}}{\partial \theta_0}\right)_{\mathscr{D}} = \mathbf{R}^{\theta} - \frac{\hat{\mathbf{n}}.\mathbf{R}^{\theta}}{\hat{\mathbf{n}}.\hat{\mathbf{x}}}\hat{\mathbf{x}}, \tag{85}$$

which may be written as

$$\left(\frac{\partial \mathbf{x}}{\partial \theta_0}\right)_{\mathscr{D}} = \frac{\hat{\mathbf{n}} \times (\mathbf{R}^{\theta} \times \hat{\mathbf{x}})}{\hat{\mathbf{n}}.\hat{\mathbf{x}}}. \tag{86}$$

It is also necessary to evaluate $\partial \hat{\mathbf{n}}/\partial \mathbf{x}$ by differentiating

$$\hat{\mathbf{n}} = \nabla G / |\nabla G|. \tag{87}$$

A few calculations lead to $\partial \hat{\mathbf{n}}/\partial \mathbf{x} = |\nabla G|^{-1}(\mathbf{I} - \hat{\mathbf{n}}\hat{\mathbf{n}}.)\nabla\nabla G.$ (88)

Thus the jump condition for the conjugate elements is slightly more complicated than those derived previously for $\boldsymbol{\nu}$, $\hat{\mathbf{x}}$, $\mathbf{p}$ and $\mathbf{R}$.

The last term in (81) has the order of magnitude of the principal curvatures of the reflecting surface. It may be neglected if the curvature is vanishingly small. In that case

$$\mathbf{Q}_2 = \mathbf{Q}_1 - 2(\mathbf{Q}_1.\hat{\mathbf{n}})\hat{\mathbf{n}} \tag{89}$$

and the quantities $\mathbf{p}$, $\boldsymbol{\nu}$, $\hat{\mathbf{x}}$, $\mathbf{R}$ and $\mathbf{Q}$ all exhibit the same kind of discontinuity.

Up to now we have assumed that the flow velocity remains finite at the wall. In reality a boundary layer forms and the flow velocity changes rapidly and vanishes at the surface. In general the boundary-layer thickness is much smaller than the acoustic wavelength of interest and the fine-structure of the velocity profile in this region does not produce a significant deviation of the characteristic rays. Therefore it is not necessary to simulate the flow field in the boundary layer. One may simply assume that the free-stream velocity is also the velocity at the boundary.

7. Examples of applications

Our aim in this section is to illustrate some of the possibilities of the geometrical technique. For this purpose we selected some problems of current interest in aeroacoustics. Other applications are described in Candel (1975, 1976*a*, *b*) and Candel, Guedel & Julienne (1975, 1976). Other attempts to use the geometrical approximation to deal with aeroacoustic problems have been made in the past by Csanady (1966), Schubert (1972) and Belleval *et al.* (1975). Schubert's and Csanady's work relies on analytical expressions of Blokhintsev's principle of conservation of acoustic energy and the treatment requires use of the geometrical solution in the far field. This approach is questionable in that the geometrical solution becomes invalid beyond the diffraction limit. A recent attempt to overcome this difficulty is presented by Balsa (1976).

In the present work we construct the geometrical solution numerically and the

field amplitude may be calculated at all distances within the diffraction limit, providing the pressure distribution in the geometric near field.

Acoustic radiation from a hot subsonic jet

This problem is relevant to the study of high frequency jet noise radiation and to the analysis of propagation of internal noise from the nozzle exit plane through the jet. We consider a jet issuing from a convergent circular nozzle at an initial speed of 390 m/s and a static temperature of 870 °K (this operating regime was selected because it had been extensively used at ONERA for basic noise research).

The mean aerodynamic jet structure has been determined by classical methods. By making use of the similarity properties of the initial and developed regions it is possible to simulate the complete structure analytically: for this we write the velocity and temperature ratios in the form

$$\frac{\Delta U}{\Delta U^0} = \frac{U - U_2^0}{U_1^0 - U_2^0} = \frac{1}{2}\left[1 + \tanh \frac{R_U}{\delta_U}\left(\frac{R_U}{r} - \frac{r}{R_U}\right)\right], \tag{90}$$

$$\frac{\Delta T}{\Delta T^0} = \frac{T - T_2^0}{T_1^0 - T_2^0} = \frac{1}{2}\left[1 + \tanh \frac{R_T}{\delta_T}\left(\frac{R_T}{r} - \frac{r}{R_T}\right)\right]. \tag{91}$$

These radial profiles are complemented by the axial variation of the shear-layer thicknesses δ_U and δ_T, the jet radii R_U and R_T and the decay laws for the velocity and temperature on the jet centre-line:

$$\Delta U^0 = \Delta U^0(x_1), \quad \Delta T = \Delta T^0(x_1). \tag{92}$$

The preceding representation accurately describes the initial jet region but some precision is lost in the developed region, where the radial profiles (90) and (91) exhibit a broader peak than the experimental distributions. Nevertheless we adopt this description for its simplicity and because it retains most of the features of the mean aerodynamic field encountered in jet flows.

Figure 3 shows a few typical profiles for the index N and Mach number M traced for the axial sections $x_1 = 0{\cdot}5D$, $1{\cdot}5D$, $3D$ and $5D$ (D = initial jet diameter). The reference sound speed c_0 appearing in the numerator of the index is that of the outer region surrounding the jet. The index is equal to unity in that region and decreases towards the jet centre-line. The mean aerodynamic structure is axisymetric and exhibits strong gradients in the radial direction and slower axial variations. The medium is not stratified and the Descartes–Snell law does not apply. In any event this law, which facilitates analytical studies of geometrical propagation, provides only marginal simplifications in the numerical calculation of the geometric field and we prefer to perform the computations without reduction of the degree of generality.

Let us first consider the radiation of wave trains from a point situated on the jet axis (in our example $x_1 = 2D$, $x_2 = 0$, $x_3 = 0$). It is easy to show that the characteristic lines are plane trajectories (see, for instance, Candel 1976*a*, *b*); they are traced on figures 4 (*a*) and (*b*) in the x_1, x_2 plane ($\alpha = 0$) for a uniform distribution of initial wave-vector directions. The angular increment separating two successive wave vectors is $\Delta\theta_0 = 10°$. The ray lines are straight in the uniform regions and exhibit a finite curvature in the regions where the velocity and temperature gradients are non-zero.

Downstream the trajectories become concave towards the outer region. In the

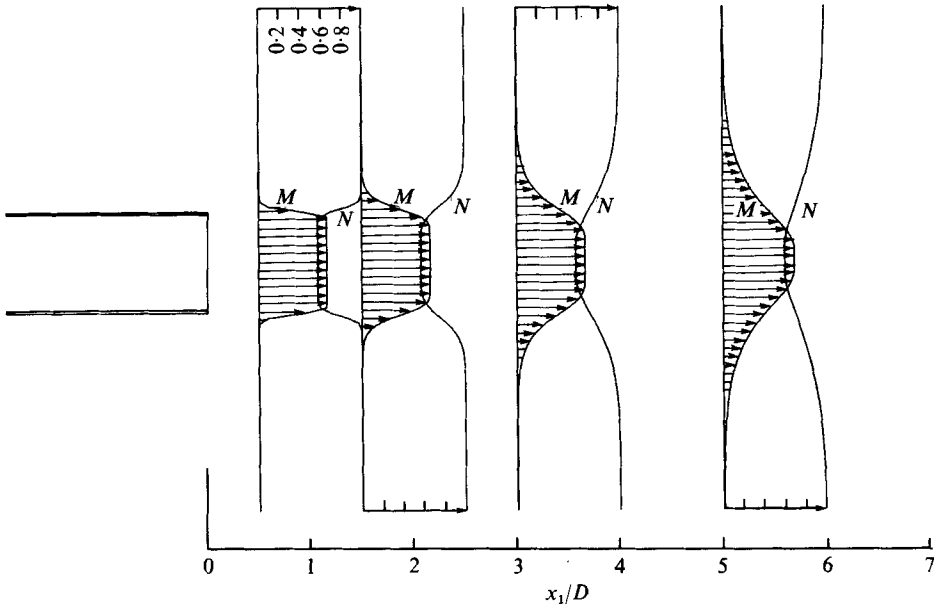

FIGURE 3. Aerodynamic mean field of a hot subsonic jet. The radial profiles of the Mach number M and index N are represented for four axial sections: $x_1 = 0{\cdot}5D$, 1·5D, $3D$ and $5D$. $U_1^0 =$ 390 m/s, $T_1^0 = 870$ °K, $U_2^0 = 0$, $T_2^0 = 283$ °K.

upstream region the rays bend towards the axis and certain characteristic lines exhibit large curvatures and are trapped inside the jet flow. In this situation the geometrical representation becomes inaccurate as a large amount of acoustic energy abandons the ray tube and is diffracted into the outer region. Figure 4 (a) also shows that the ray-tube cross-section changes rapidly in the downstream direction (around $\theta \sim 30°$) and from this observation we anticipate a decrease in the field amplitude in that region. In addition we notice that, after the initially rapid increase in the ray-tube section, the ray beam expands very slowly in the downstream region. If we were to compute the field amplitude at a large distance from the jet, this would lead to a very large amplitude. However, because of wave diffraction the geometric solution is limited in range and should not be applied to calculate the far field. For this reason we are going to calculate the field amplitude at a finite distance from the source in a region we call the geometric near field. This point is worth further discussion.

We distinguish three different domains in the case of acoustic radiation from an inhomogeneous region:

(i) the hydrodynamic near field, which extends to about one wavelength from the source;

(ii) the geometric near field, which is bounded in range by the diffraction limit ($r < r_D$);

(iii) the far field, which lies beyond the diffraction limit ($r > r_D$).

In the case of radiation from an aperture having a diameter D the diffraction limit is known to be $r_D \sim D^2/\lambda$. For radiation from an inhomogeneous medium the 'effective diffraction aperture' is not defined rigorously but we may infer that it is proportional to a characteristic scale of the flow field and that it depends on the degree of

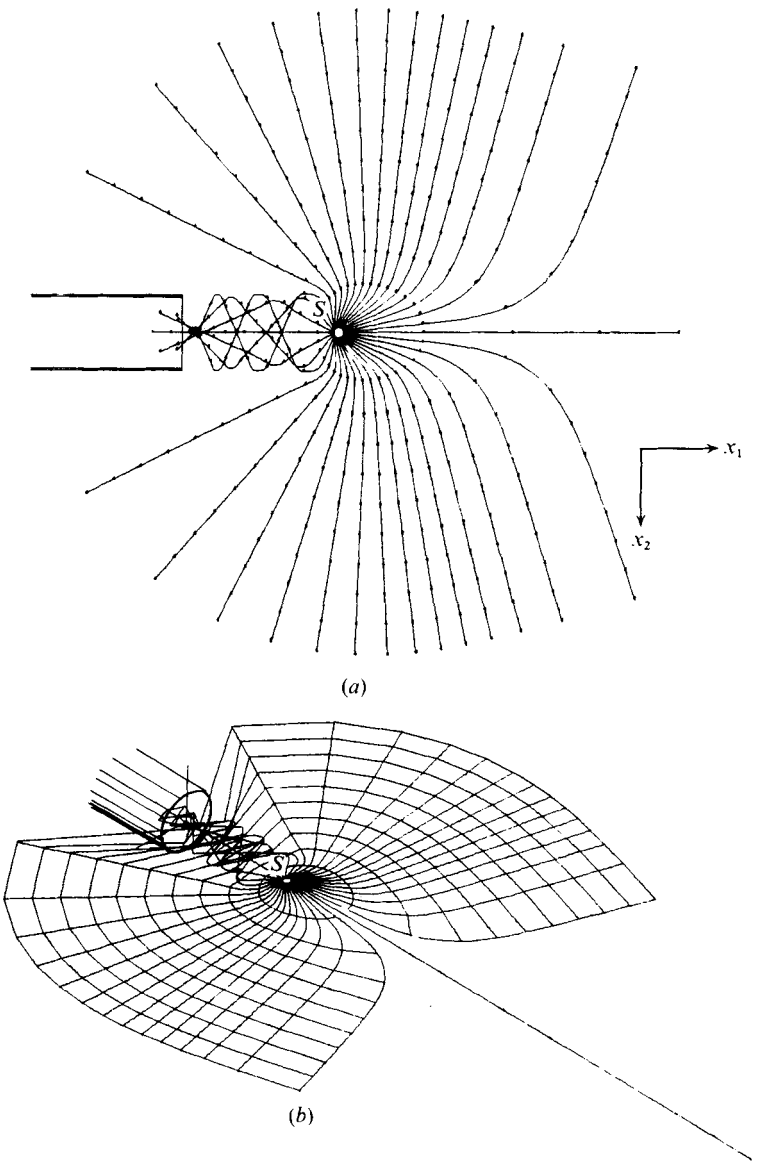

FIGURE 4. Typical ray tracing. Aerodynamic conditions as in figure 3 with the source at $x_1^0 = 2D$, $x_2^0 = 0$, $x_3^0 = 0$. (*a*) Plan view. (*b*) Isometric perspective showing the position of successive phase fronts.

inhomogeneity. Thus $$r_D \sim f(\delta N_G/N_G) D^2/\lambda, \tag{93}$$

where f is an unknown function which decreases when $\delta N_G/N_G$, the relative variation of the generalized index, increases. The distinction between the geometric near field and the far field is not generally taken into account and numerous studies based on the geometrical approximation use the geometrical solution to calculate the far-field radiation. This leads in many cases to physically unacceptable results. For this reason we shall only use the geometrical algorithm to calculate the near-field amplitude.

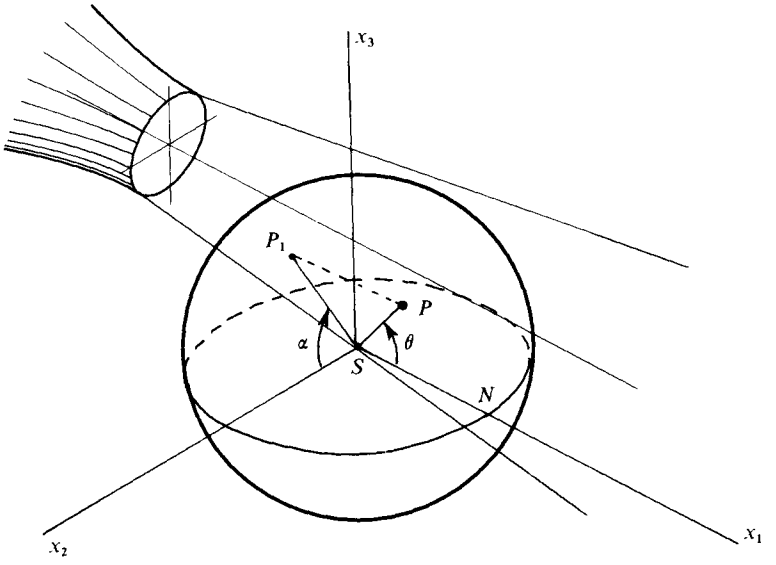

FIGURE 5. Observation sphere. The sphere is centred on the source and the x_1 axis is parallel to the jet axis. $\theta = (Sx_1, SP)$, $\alpha = (Sx_2, SP_1)$.

Now a convenient way to represent the effects of refraction on the radiated sound field is to define a transmission ratio

$$T(\alpha, \theta; \mathbf{r}_2, \mathbf{r}_1) = \frac{\Pi_0(\mathbf{r}_2)}{\Pi_0(\mathbf{r}_1)} \frac{r_2}{r_1}; \tag{94}$$

this ratio is calculated between two points $\mathbf{r}_1$ and $\mathbf{r}_2$ lying on the same ray. The first point $\mathbf{r}_1$ is situated in the vicinity of the source while the point $\mathbf{r}_2$ is located on a 'sphere of observation' centred on the source. The radius of this sphere is of the order of a few nozzle diameters, so that the observation points may be considered to lie in the geometric near field (figure 5). To allow a planar mapping of the sphere we define the angular co-ordinates θ and α with respect to a Cartesian system whose origin coincides with the source:

θ ($-180° < \theta \leqslant +180°$) is a latitude measured with respect to OX_1;

α ($-90° < \alpha \leqslant 90°$) is a longitude which designates the angle between the axial plane passing through the point of observation $\mathbf{r}_2$ and the horizontal axis OX_2.

The transmission ratio defined by (94) contains a factor r_2/r_1 which compensates for the spherical divergence effect. When the propagation medium is uniform or at rest, the transmission coefficient becomes unity. In a region where the gradients are non-vanishing the transmission ratio differs from unity and thus characterizes the effects associated with refraction.

Figure 6 presents the transmission coefficient corresponding to the ray tracing in figures 4(*a*) and (*b*). The calculations were performed between points situated on a small sphere $r_1 = 0{\cdot}1D$ near the source and the points on the observation sphere $r_2 = 3D$. The coefficient is less than unity (0 dB) in the downstream ($\theta \sim 30°$) and upstream ($\theta \sim 120°$) regions. It exceeds unity in the forward region around $\theta \sim 60°$ and exhibits a maximum of about 4·4 dB. The distribution appears 'heart shaped'

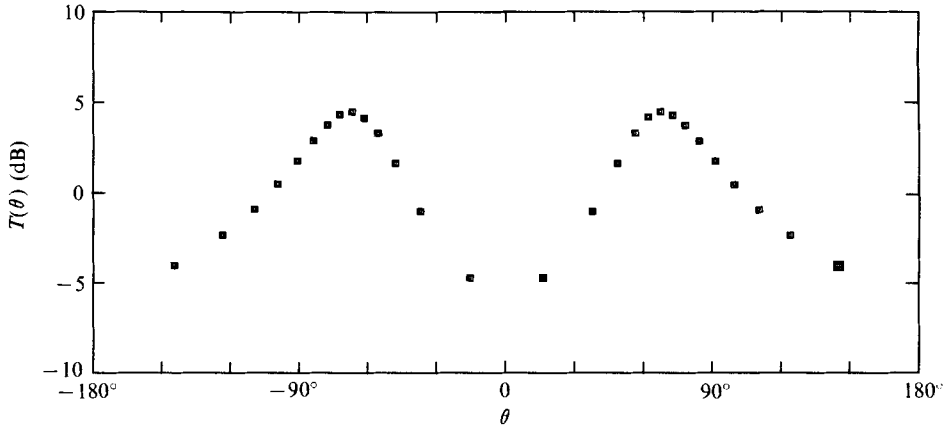

FIGURE 6. Transmission-coefficient distribution corresponding to the ray tracing in figure 4(*a*). $r_1 = 0{\cdot}1D$, $r_2 = 3D$. A unit transmission coefficient is represented by 0 dB.

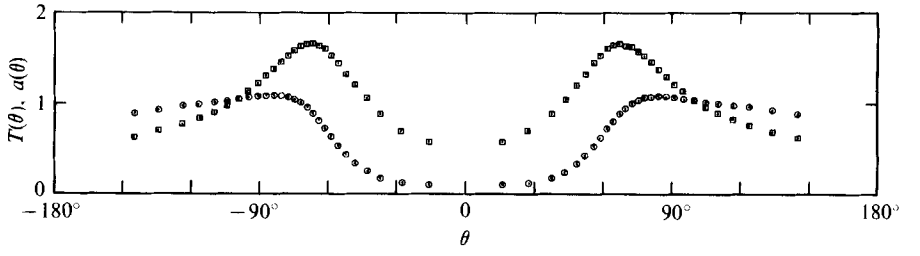

FIGURE 7. Geometrical expansion coefficient a (circles) and transmission coefficient T (squares) corresponding to the ray tracing in figure 4(*a*). $r_1 = 0{\cdot}1D$, $r_2 = 3D$.

and resembles the radiation patterns characteristic of jet noise. This feature becomes particularly evident if the transmission-coefficient distribution is compared with the radiation diagrams of jet noise traced for the higher frequency bands. This comparison is carried out in Candel (1976*b*) and it is shown that for a $\frac{1}{3}$-octave centred on the Strouhal number $St = 5$ (i.e. for $fD/U_1^0 = 5$) the calculated and experimental diagrams coincide almost exactly. We refer the reader to this reference for further discussion of this point.

Now, to allow some interpretation of figure 6, we give in figure 7 the distribution of the 'divergence or geometrical expansion coefficient', defined as the ratio

$$a = \frac{\delta\Sigma_2}{\delta\Sigma_1}\frac{r_1^2}{r_2^2}. \tag{95}$$

This ratio differs from unity when the wave-front elementary area ceases to be proportional to the square of the distance to the source. This deviation, evidently related to refraction, occurs in particular in the downstream region, in the neighbourhood of the jet axis. In that region we have already noticed that the ray-tube cross-section grows more rapidly than the square of the polar distance. In other words, the ray tube expands rapidly and the amplitude diminishes as a consequence of the conservation principle (19).

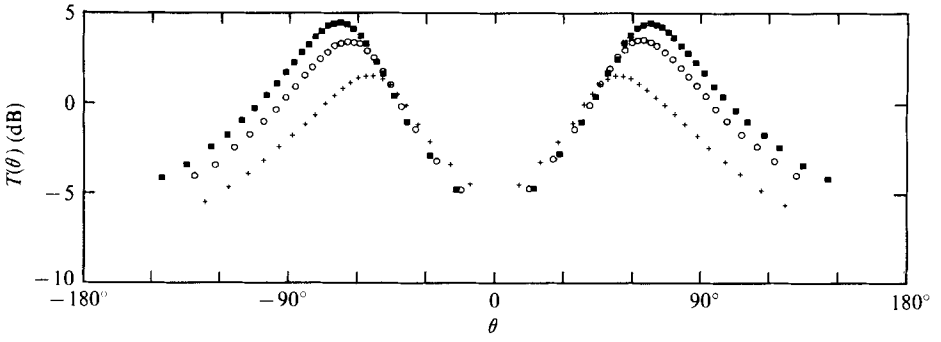

FIGURE 8. Variation of the transmission coefficient with the jet temperature for a constant Mach number. $x_1^0 = 2D$, $x_2^0 = 0$, $x_3^0 = 0$. ■, $U_1^0 = 390$ m/s, $T_1^0 = 870$ °K; ○, $U_1^0 = 323$ m/s, $T_1^0 = 600$ °K; +, $U_1^0 = 228$ m/s, $T_1^0 = 300$ °K.

We note, in contrast, that in the upstream region the wave-front area nearly increases like the distance squared ($a \sim 1$). This time the amplitude diminishes as a direct consequence of the presence of the flow. This may be seen by returning to the conservation principle (19). The conserved quantity is the flux integrated over the ray-tube cross-section (appendix B):

$$(\Pi_0^2/\rho c)(1+\mathbf{M}.\boldsymbol{\nu})|\boldsymbol{\nu}+\mathbf{M}|\,\delta a. \tag{96}$$

By making use of
$$\delta a = \delta\Sigma(1+\mathbf{M}.\boldsymbol{\nu})/|\boldsymbol{\nu}+\mathbf{M}| \tag{97}$$

expression (96) may be rewritten in the form

$$(\Pi_0^2/\rho c)(1+\mathbf{M}.\boldsymbol{\nu})^2\,\delta\Sigma. \tag{98}$$

Now if the cross-section $\delta\Sigma$ grows like distance squared the conservation of (98) implies that
$$\Pi_0 r \sim c^{-\frac{1}{2}}(1+\mathbf{M}.\boldsymbol{\nu})^{-1} \sim T^{-\frac{1}{2}}(1+\mathbf{M}.\boldsymbol{\nu})^{-1}. \tag{99}$$

The product $\Pi_0 r$ varies like the temperature to the power $-\frac{1}{4}$ and also like the reciprocal of the factor $1+\mathbf{M}.\boldsymbol{\nu}$. For a wave vector directed upstream, $1+\mathbf{M}.\boldsymbol{\nu}$ increases from the interior to the exterior of the jet and the product $\Pi_0 r$ decreases, explaining the behaviour of the transmission ratio in the upstream region. The temperature dependence is also exhibited by the calculated transmission coefficients in figure 8. The temperature is varied while keeping the initial Mach number constant and equal to 0·69. The maximum value of the transmission ratio decreases when the temperature decreases and the position of the maximum shifts towards the jet axis. In the downstream region $|\theta| < |\theta_{\max}|$ the transmission coefficient depends weakly on the temperature. Upstream it increases like $T^{\frac{1}{4}}$.

To complete this analysis of radiation from the jet axis we present a plot (figure 9) of the successive wave fronts associated with the ray trajectories in figure 4(*a*). Between each wave front the parameter S/D is incremented by $\Delta S/D = 0{\cdot}4$ and the corresponding propagation time may be found from

$$\Delta\tau = \Delta S/c_0 = 0{\cdot}4D/c_0. \tag{100}$$

The initially spherical phase fronts are convected by the inner jet flow and distorted in the shear region. Their final appearance is that of a heart.

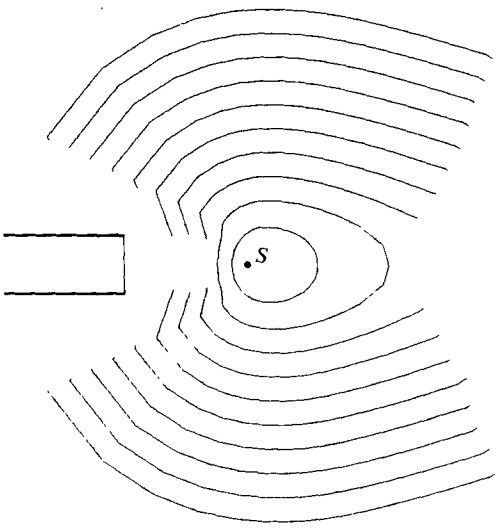

FIGURE 9. Wave fronts for the ray tracing in figure 4(*a*).

Acoustic radiation from a nozzle exit

This second example is of interest in the case of engine core noise radiation. The problem was treated previously by, for instance, Mani (1973), who assumed modal propagation and a plug flow to represent the jet. Our purpose being strictly illustrative, we consider the simplest situation of a point source radiating from inside a channel containing a uniform flow. At the end of the channel we assume that a free-jet type of flow is formed.

A ray tracing corresponding to this situation appears on figure 10. Certain rays propagate directly towards the external region. Others are first reflected by the channel walls before escaping from the channel. Upon refraction by the jet flow, some of these rays are directed towards the upstream region and reach points situated in the shadow of the channel walls. These particular rays correspond to waves emitted by the source with a wave vector oriented upstream but convected downstream by the uniform flow.

The transmission-coefficient distribution corresponding to this situation is shown on figure 11. It exhibits two branches, the first corresponds to the direct rays, the second to the rays undergoing a single reflexion. The discontinuity which exists between the two branches is essentially due to the difference in arc length between the direct and reflected rays. In reality the discontinuities exhibited by the geometrical field are compensated by a diffracted field. However the diffracted field is not calculated by the present algorithm.

Three-dimensional refraction by a jet flow

Three-dimensional refraction effects have not been analysed extensively in the past. They may be of considerable importance in the case of flows which are not axisymmetric (elliptical, rectangular or notched nozzles). More generally, such effects arise when the radiation originates from a point situated off the jet axis. This case is analysed here.

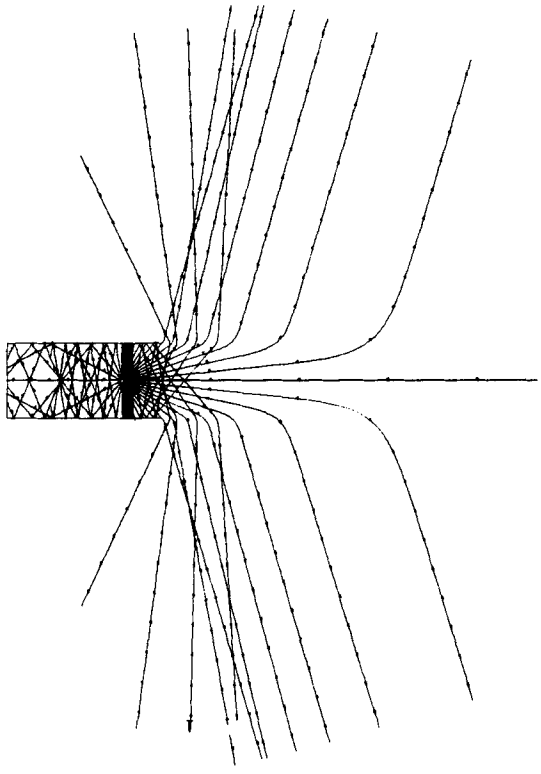

FIGURE 10. Ray tracing for a source situated inside the nozzle. Aerodynamic conditions as in figure 3.

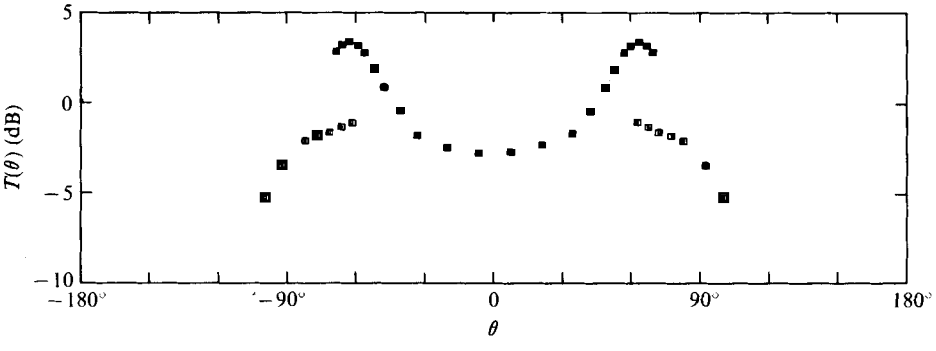

FIGURE 11. Transmission coefficient corresponding to figure 10. $r_1 = 0{\cdot}1D$, $r_2 = 3D$. ■, direct rays; ⊡, reflected rays.

A first three-dimensional effect is made evident by the ray tracing for a source placed off the jet axis. This is exemplified by figures 12(*a*)–(*c*). The rays are launched in a horizontal plane and the source is situated above the jet axis at $x_1^0 = 6D$, $x_2^0 = 0$, $x_3^0 = 0{\cdot}6D$. The rays escape from the initial emission plane and clearly appear as three-dimensional trajectories. Further evidence is provided by figures 13(*a*)–(*c*), which show the ray tracing for a source situated in the horizontal plane and an initial emission plane $\alpha_0 = 45°$ parallel to the jet axis.

Now, by varying the initial angle α_0 and plotting the points of intersection of the ray families with the sphere of observation we obtain a first set of contours (figure 14). These contours curve away from the initial emission planes ($\alpha_0 = 30$, 45, 60, 75 and 90°), which would appear as horizontal lines on figure 14. We note that in the right hemisphere (the hemisphere situated on the source side of the jet axis) the rays penetrate the sphere, below the emission plane in the downstream region and above that plane in the upstream direction. The inverse effect is observed in the left hemisphere. All the contours have a common point in the right hemisphere corresponding to the ray whose initial wave vector is parallel to the jet axis ($\theta_0 = 0$).

Figure 14 also displays the contours of constant transmission coefficient. A strong maximum appears in the right hemisphere ($+7{\cdot}4$ dB) in the horizontal plane $\alpha = 0$ at about $\theta = 66°$. The transmission coefficient remains greater than unity in an elongated domain surrounding that point and extending beyond $\alpha = 90°$ into the left hemisphere. There the coefficient exhibits a local maximum of 2·4 dB at $\alpha = 0$ and $\theta \sim -67°$ but its value is greater near the poles $\alpha = \pm 90°$, where it exceeds unity by about 3·1 dB. This map shows that the jet acts as a partial shield for radiation in the left hemisphere while it enhances the field amplitude in the right hemisphere. This behaviour may be essentially ascribed to geometrical modifications of the ray tubes.

The region surrounding the jet axis ($\theta = 0$) is reached by a small number of 'exceptional' rays with a reduced transmission coefficient. In this way a region of silence forms, bounded by $\theta \sim 35°$ in the right hemisphere and by $\theta \sim -30°$ in the left hemisphere. This region is approximately conical with a half-angle of about 30°. In reality diffraction and scattering effects prevent the formation of a region of vanishing amplitude. The transition between the region where the transmission coefficient reaches its maximum and the neighbourhood of the jet axis is also more gradual than is predicted by the geometrical approximation.

To conclude this section, it is worth comparing the present results with those obtained in the case of radiation from the jet axis. This comparison is simplified by plotting the transmission coefficient of figure 6 as contours on the observation sphere (figure 15). In this representation the contours appear as vertical (θ = constant) lines. The transmission coefficient reaches a maximum of 4·4 dB above unity at $\theta \sim \pm 67°$ and a region of silence exists in a downstream cone having a half-angle of 30° and surrounding the jet axis. The deformation of the transmission-coefficient distribution is made apparent by comparing figures 14 and 15.

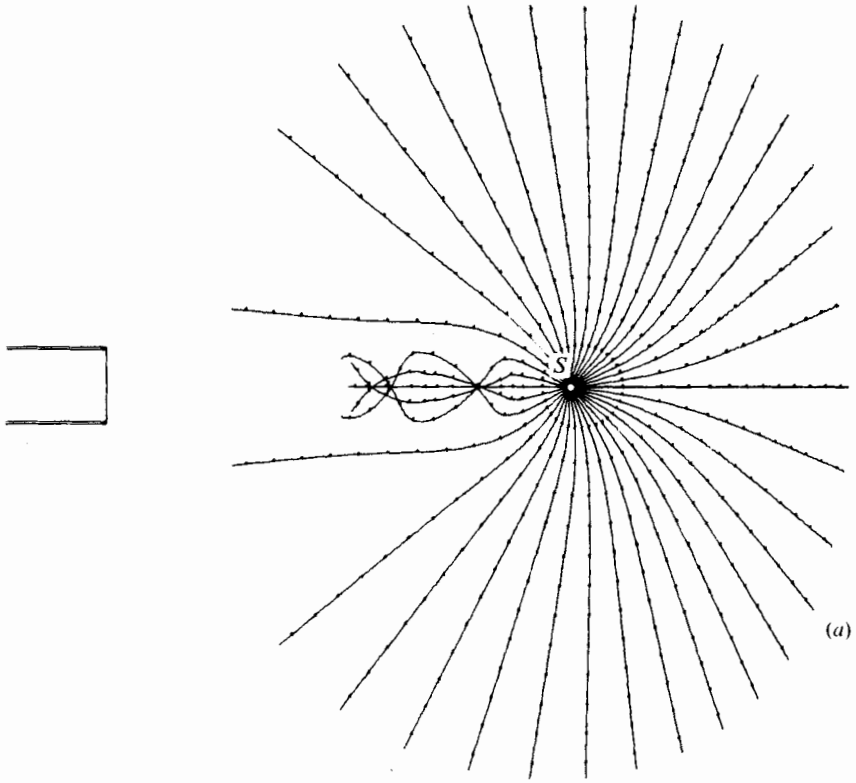
S
(a)

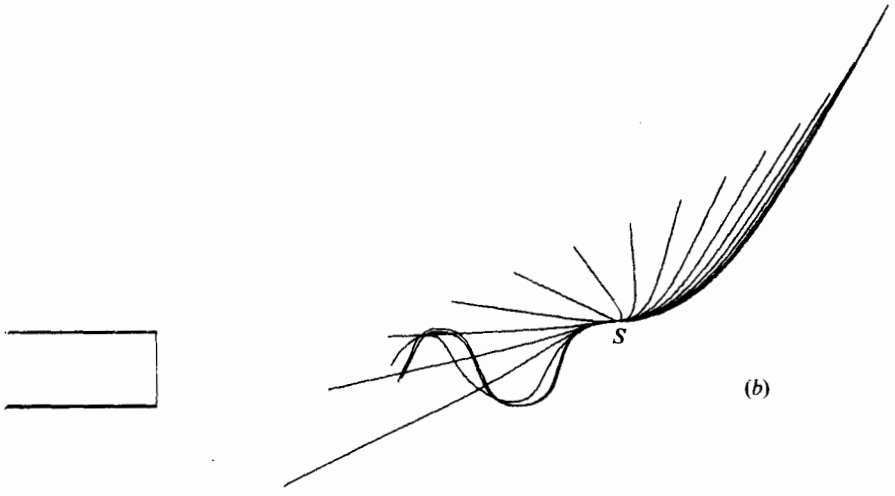
S
(b)

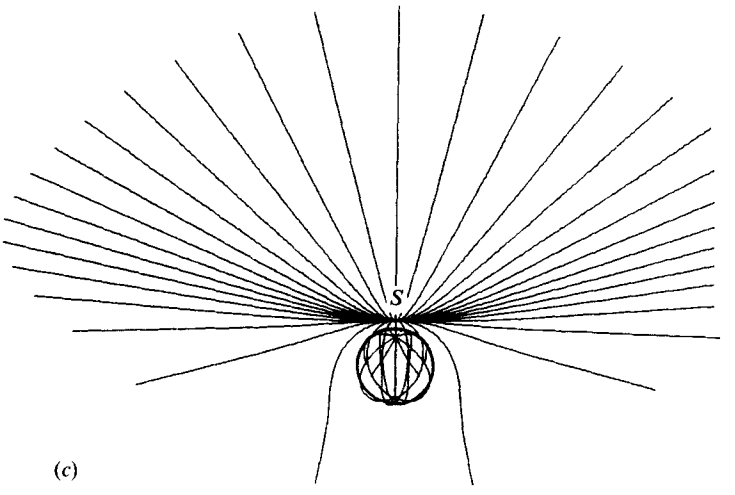

FIGURE 12. Ray tracing for a source situated off the jet axis at $x_1^0 = 6D$, $x_2^0 = 0$, $x_3^0 = 0{\cdot}6D$. Rays emitted in the $\alpha_0 = 0$ plane. (*a*) Projection on x_1, x_2 plane. (*b*) Projection on x_1, x_3 plane. (*c*) Projection on x_2, x_3 plane.

8. Concluding remarks

We have developed in this paper a method for solving the conservation equations describing the propagation of linear waves in slightly inhomogeneous and dispersive media. The method, based on differentiation of the characteristic system with respect to the initial parameter space, is well suited for numerical implementation. The method also applies to cases where the field is reflected by solid boundaries. This has been achieved by deriving a set of jump conditions which serve to re-initiate the numerical integration when a reflexion occurs.

The numerical algorithm thus allows the treatment of fairly general problems and its possibilities have been illustrated by analysing a few examples of importance in aeroacoustics.

We note however that the computation cannot be performed in the vicinity of caustics. There the ray-tube cross-section vanishes and the field amplitude becomes infinite. The first-order geometrical solution breaks down under these conditions. The method does not apply either to cases of nonlinear propagation where the ray-tube area depends on the wave amplitude itself. However an extension to this case seems possible.

This paper is part of a Doctorat d'Etat to be presented at Université de Paris VI. A preliminary version was presented at the 14th International Congress of Theoretical and Applied Mechanics, Delft, 1976. The author thanks Professor Pierre Alais and Professor Mariano Perulli for their constant support during the preparation of this work. He also gratefully acknowledges helpful discussions with Professor Jean Pierre Guiraud.

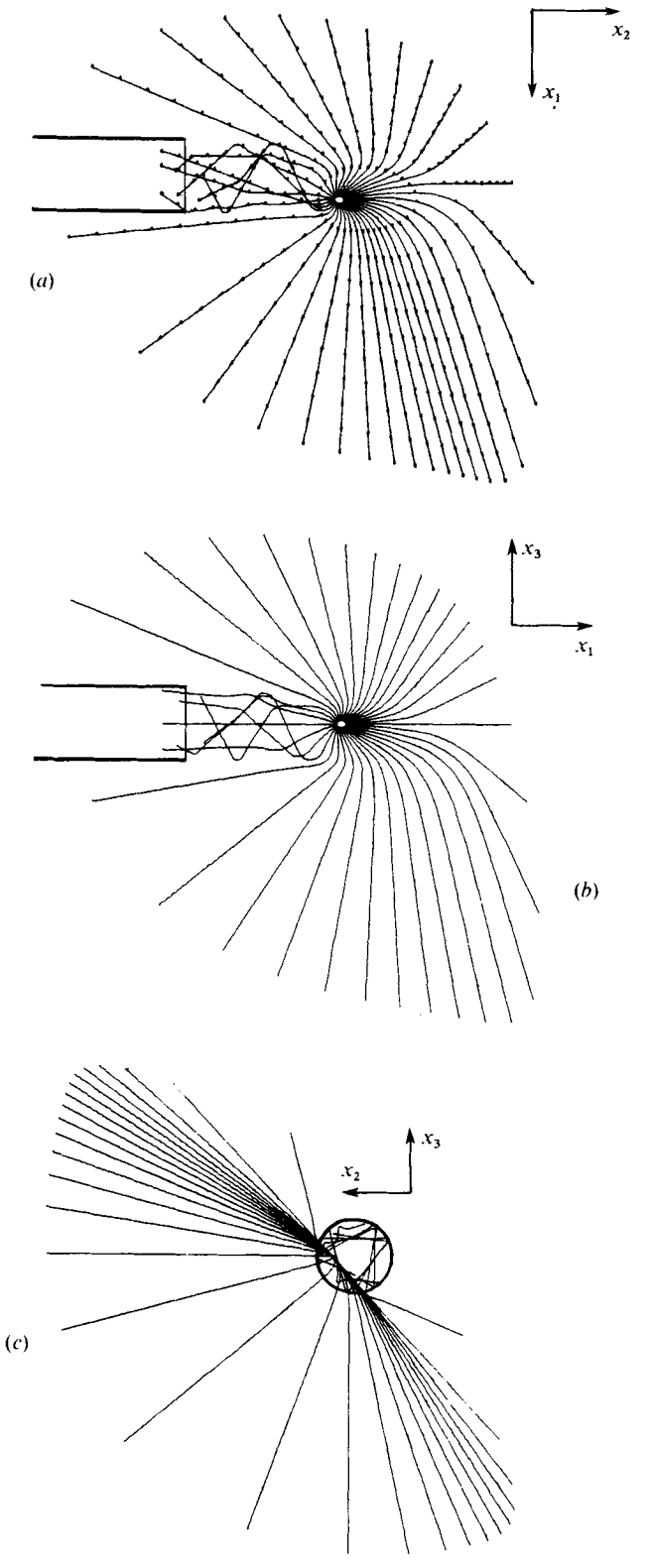

FIGURE 13. Ray tracing for a souree situated off the jet axis at $x_1^0 = 2D$, $x_2^0 = 0{\cdot}3D$, $x_3^0 = 0$. Rays are emitted in the $\alpha_0 = 45°$ plane. (*a*) Projection on x_1, x_2 plane. (*b*) Projection on x_1, x_3 plane. (*c*) Projection on x_2, x_3 plane.

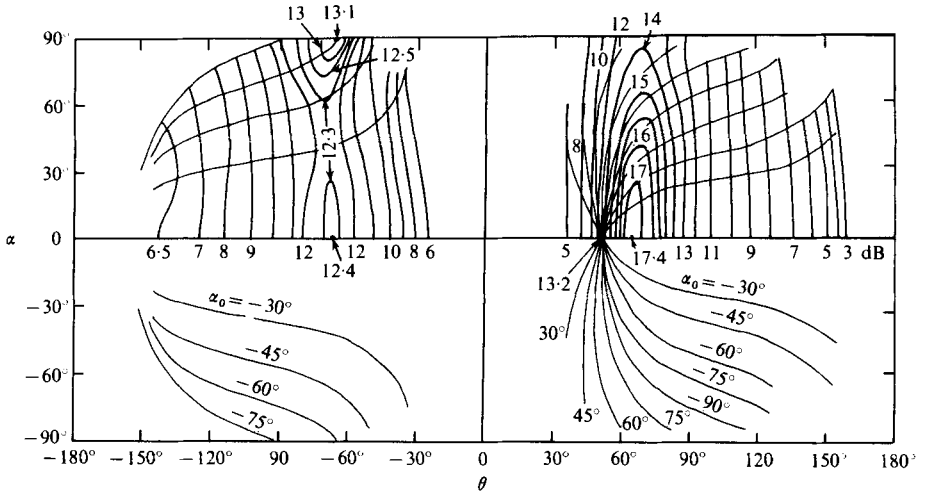

FIGURE 14. Contours of transmission coefficient and lines of penetration of rays into the observation sphere. $x_1^0 = 2D$, $x_2^0 = 0{\cdot}3D$, $x_3^0 = 0$, $r_1 = 0{\cdot}1D$, $r_2 = 3D$. Aerodynamic conditions as in figure 3. A unit transmission coefficient is represented by 10 dB.

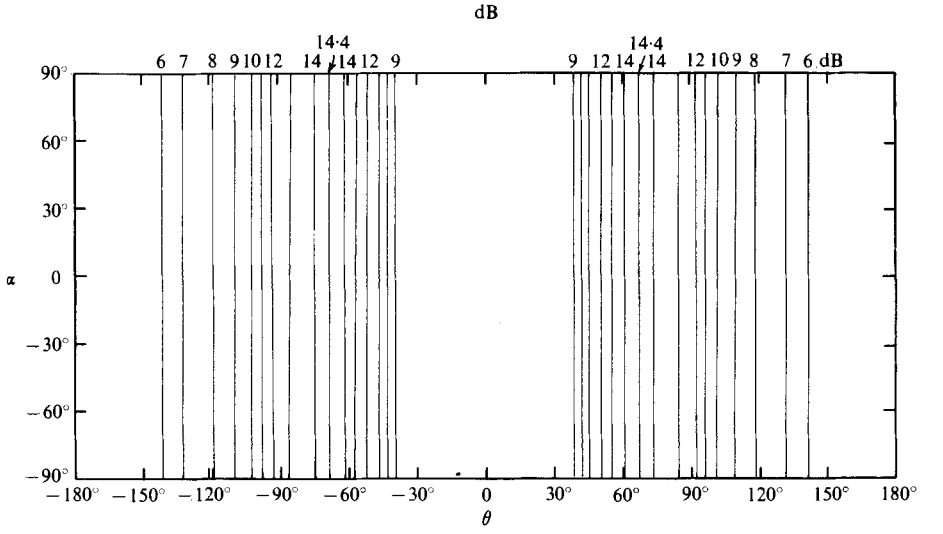

FIGURE 15. Contours of transmission coefficient for radiation from the jet axis $x_1^0 = 2D$, $x_2^0 = 0$, $x_3^0 = 0$ (as in figure 6). A unit transmission coefficient is represented by 10 dB.

Appendix A

In table 1 we summarize the first-order geometrical acoustics theory for a time-dependent medium (Guiraud 1965; Hayes 1968; Bretherton & Garrett 1968; Lighthill 1972).

Π = pressure	$\boldsymbol{\xi}$ = velocity	σ = entropy
Field description	$\begin{bmatrix}\Pi\\ \boldsymbol{\xi}\\ \sigma\end{bmatrix} = \begin{bmatrix}\Pi_0\\ \boldsymbol{\xi}_0\\ \sigma_0\end{bmatrix} \exp\{i\psi(\mathbf{x},t)\}$	$\boldsymbol{\xi} = \dfrac{\boldsymbol{\nu}}{\rho c}\Pi_0$ $\sigma_0 = 0$
Dispersion relation	$\omega = kc + \mathbf{k}.\boldsymbol{\nu} = kc(1+\mathbf{M}.\boldsymbol{\nu})$	
Group velocity	$\mathbf{c}_g = c\boldsymbol{\nu} + \boldsymbol{\nu} = c(\boldsymbol{\nu}+\mathbf{M})$	
Ray equations	$d^c\mathbf{x}/dt = \boldsymbol{\nu} + c\boldsymbol{\nu}$ $d^c\mathbf{k}/dt = -k\nabla c - \nabla\boldsymbol{\nu}.\mathbf{k}$ $d^c\omega/dt = k\,\partial c/\partial t + \mathbf{k}.\partial\boldsymbol{\nu}/\partial t$ $d^c\psi/dt = 0$	
Wave action	$A_0 = \dfrac{\Pi_0^2}{\rho c^2}\dfrac{1}{kc} = \dfrac{\Pi_0^2}{\rho c^2}\dfrac{1+\mathbf{M}.\boldsymbol{\nu}}{\omega}$	
Conservation equation	$\partial A_0/\partial t + \nabla.\mathbf{c}_g A_0 = 0$	

TABLE 1

Appendix B

In table 2 we summarize the first-order geometrical acoustics theory for a time-independent medium (Blokhintsev 1946; Keller 1954).

Field description	$\begin{bmatrix}\Pi\\ \boldsymbol{\xi}\\ \sigma\end{bmatrix} = \begin{bmatrix}\Pi_0\\ \boldsymbol{\xi}_0\\ \sigma_0\end{bmatrix} \exp(ik_0S - i\omega t)$	$\boldsymbol{\xi}_0 = \dfrac{\boldsymbol{\nu}}{\rho c}\Pi_0$ $\sigma_0 = 0$
Eikonal equation	$(\nabla S)^2 = (N - \mathbf{M}.\nabla S)^2$	$\mathbf{p} = \nabla S$ $p = N/(1+\mathbf{M}.\boldsymbol{\nu})$
Group velocity	$\mathbf{c}_g = c(\boldsymbol{\nu}+\mathbf{M})$	
Ray equations	$d^c\mathbf{x}/dS = N^{-1}(\boldsymbol{\nu}+\mathbf{M})$ $d^c\mathbf{p}/dS = N^{-1}[\nabla N - (\nabla\mathbf{M}).\mathbf{p}]$	
Energy density	$E_0 = (\Pi_0^2/\rho c^2)(1+\mathbf{M}.\boldsymbol{\nu}) = A_0\omega$	
Conservation equation	$\nabla.\mathbf{c}_g E_0 = 0$	

TABLE 2

REFERENCES

BALSA, T. F. 1976 Refraction and shielding of sound from a source in a jet. *J. Fluid Mech.* **76**, 443.

BELLEVAL, J. F. DE, RANDON, J., PERULLI, M. & TAILLEFESSE, J. C. 1975 Influence of refraction effects on the interpretation of hot jet acoustic radiation. *Prog. Astronaut. Aeronaut.* **37**, 93.

BLOKHINTSEV, D. I. 1946 Acoustics of a non homogeneous moving medium. *N.A.S.A. Tech. Memo.* no. 1399.

BORN, M. & WOLF, E. 1975 *Principles of Optics*, 5th ed. Pergamon.

BRETHERTON, F. P. & GARRETT, C. G. R. 1968 Wave trains in inhomogeneous moving media. *Proc. Roy. Soc.* A **302**, 529.

CANDEL, S. M. 1975 Acoustic conservation principles and an application to plane and modal propagation in nozzles and diffusers. *J. Sound Vib.* **41**, 207.

CANDEL, S. M. 1976*a* Application of geometrical techniques to aeroacoustic problems. *A.I.A.A. Paper*, no. 76-546.

CANDEL, S. M. 1976*b* Etudes théoriques et expérimentales de la propagation acoustique en milieu inhomogène et en mouvement. Thèse de Doctorat d'Etat, Université de Paris VI.

CANDEL, S. M., GUEDEL, A. & JULIENNE, A. 1975 Refraction and scattering in an open wind tunnel flow. *Proc. 6th Int. Cong. Instrumentation in Aerospace Simulation Facilities, Ottawa*, p. 288.

CANDEL, S. M., GUEDEL, A. & JULIENNE, A. 1976 Radiation, refraction and scattering of acoustic waves in a free shear flow. *A.I.A.A. Paper*, no. 76-544.

CHEN, D. C. & LUDWIG, D. 1973 Calculation of wave amplitudes by ray tracing. *J. Acoust. Soc. Am.* **54**, 431.

CSANADY, G. T. 1966 The effect of mean velocity variation on jet noise. *J. Fluid Mech.* **26**, 183.

FELSEN, L. & MARCUVITZ, N. 1970 *Radiation and Scattering of Waves*. Prentice Hall.

FOCK, V. A. 1965 *Electromagnetic Diffraction and Propagation Problems*. Pergamon.

FRIEDLANDER, F. G. 1958 *Sound Pulses*. Cambridge University Press.

GOSSARD, E. E. & HOOKE, W. H. 1975 *Waves in the Atmosphere*. Elsevier.

GUIRAUD, J. P. 1965 Acoustique géométrique, bruit balistique des avions supersoniques et focalisation. *J. Méc.* **4**, 215.

HAYES, W. D. 1968 Energy invariant for geometric acoustics in moving medium. *Phys. Fluids* **11**, 1654.

HAYES, W. P. 1970 Kinematic wave theory. *Proc. Roy. Soc.* A **320**, 209.

HAYES, W. P., HAEFLI, R. C. & KULSRUD, H. E. 1970 Sonic boom propagation in a stratified atmosphere with computer program. *N.A.S.A. Contractor Rep.* no. 1299.

KELLER, J. B. 1954 Geometrical acoustics. I. The theory of weak shock waves. *J. Appl. Phys.* **25**, 938.

KLINE, M. 1961 A note on the expansion coefficient of geometrical optics. *Comm. Pure Appl. Math.* **15**, 473.

LIGHTHILL, M. J. 1972 The fourth annual Fairey lecture: the propagation of sound through moving fluids. *J. Sound Vib.* **24**, 471.

MACKINNON, R. F., PARTRIDGE, J. S. & TOOLE, H. S. 1972 On the calculation of ray acoustic intensity. *J. Acoust. Soc. Am.* **52**, 1471.

MANI, R. 1973 Refraction of acoustic duct wave guide modes by exhaust jets. *Quart. Appl. Math.* **30**, 501.

MARCUSE, D. 1972 *Light Transmission Optics*. Van Nostrand.

QUEMADA, D. 1968 *Ondes dans les Plasmas*. Paris: Hermann.

SCHUBERT, L. K. 1972 Numerical study of sound radiation by a jet flow. I. Ray acoustics. *J. Acoust. Soc. Am.* **51**, 439.

SOLOMON, L. P. & ARMIJO, L. 1971 An intensity differential equation in ray acoustics. *J. Acoust. Soc. Am.* **50**, 960.

STRUBLE, R. A. 1962 *Nonlinear Differential Equations*. McGraw-Hill.

TELFORD, W. M., GELDART, L. P., SHERIFF, R. E. & KEYS, D. A. 1976 *Applied Geophysics*. Cambridge University Press.

UGINCIUS, P. 1969 Intensity equations in ray acoustics I and II. *J. Acoust. Soc. Am.* **45**, 193.

URICK, J. 1967 *Principles of Underwater Sound*. McGraw-Hill.

WHITHAM, G. B. 1974 *Linear and Nonlinear Waves*. Wiley.